Natural Resources for Human Health
eISSN: 2583-1194

Original Research

Received 29 May 2026
Revised 21 June 2026
Accepted 18 July 2026

Natural Resources for Human Health 2026, Vol. 6 (10s): 355–368

KEYWORDS:
Mathematical modelling; Organic waste drying; Empirical model; Activation Energy; Moisture Diffusivity; Energy Efficiency; Circular economy

Modeling and Analysis of Convective Drying Kinetics of Household Biodegradable Waste Using Semi-Empirical Thin Layer Models

Punam Bundele[1], Marshiana D[1]*, Adeline Sneha J[2]

[1]Electronic and Telecommunication, Symbiosis Institute of Technology, Pune Campus, Symbiosis International (Deemed University), Pune 412115, Maharashtra, India
[2]School of Computing, Asia Pacific University of Technology and Innovation, Kuala Lumpur, Malaysia

ABSTRACT: Household organic waste contains high moisture levels that hinder its efficient utilization and increase disposal costs. This study examines the convective hot-air drying characteristics of domestic organic waste at air temperatures of 70, 90, 100, 120, and 140 °C. The starting moisture content of the fresh waste was 68–75% wet basis (w.b.), and we determined its physicochemical properties using established analytical procedures. Eight established thin-layer drying models, including Newton, Henderson–Pabis, Page, Logarithmic, Midilli–Kucuk, Verma, Wang–Singh, and Two-Term, were implemented in the MATLAB environment to describe the experimental moisture ratio profiles. Model adequacy was assessed using a combination of statistical indicators, namely the coefficient of determination (R^2),root mean square error (RMSE), reduced chi-square (χ^2), Akaike information criterion (AIC), and Bayesian information criterion (BIC). Among the evaluated models, the Midilli–Kucuk model provided the closest agreement with the experimental data, achieving an $R^2$of 0.9996, an RMSE of 0.0071, and a χ^2value of 7.21×10^{-5}. The effective moisture diffusivity increased from $4.70\times 10^{-9}$to 2.60×10^{-8} m^2s^{-1}, while the activation energy was evaluated to be 27.22 kJ mol^{-1}. Energy analysis showed that 100 °C offered the optimal balance among drying time, specific energy utilization, and product quality attributes. The results confirm that the Midilli–Kucuk model is suitable to simulate the drying process of household organic waste and offer a strong basis for the optimization of energy-saving drying systems in the waste valorization process in a circular economy context.

1. INTRODUCTION

A major environmental problem of the 21st century is the rapid growth in municipal solid waste (MSW) accumulation. Global waste generation reached approximately 2.56 billion tonnes and is projected to increase to 3.86 billion tonnes in the baseline scenario by 2050 under a business-as-usual scenario [1]. The largest fraction is comprised of organic waste, which ranges from 44-60% for countries with low and middle income levels and 32% for high-income countries[2]. In India, organic waste constitutes approximately 40-60% of Municipal solid waste(MSW), and most of the organic waste comes from domestic sources [3][4]. If not managed appropriately, serious environmental impacts will arise: When waste is dumped openly and decomposes without control, it releases methane, which is responsible for nearly 20% of anthropogenic methane emissions globally [5]. Drying is an important pre-processing operation for organic waste valorization, which can be used to produce compost, biogas, animal feed, or biofertilizers [6], [7], [8]. Moisture reduction reduces waste mass by 60-80%, stops biological degradation, and increases processing efficiency downstream[9]. Hot-air convective drying is widely adopted because of its simple operation, low cost, and effective moisture removal capability, though energy costs and process optimization remain challenges. The optimized hot-air drying of red beetroot using a variable temperature profile (120–50°C) significantly reduced drying time while achieving high model accuracy (R^2 = 0.998) and Arrhenius-type moisture diffusivity behavior[10]. Drying is a dynamic process governed by concurrent heat and mass transfer between the drying medium and the material, which is dependent upon Fickian diffusion mechanisms and has strong temperature, air velocity, and material property dependency[11], [12]. The purpose of mathematical modelling of drying kinetics is threefold: to predict the moisture evolution without the need for extensive drying experiments, to optimise the use of energy and process effectiveness, and to automate the process and control it. Numerous thin-layer drying models, ranging from simple empirical to complex semi-theoretical formulations, have been proposed to describe drying behaviour, including the first-order kinetic model (Newton), the multi-parameter model (Midilli-Kucuk), and the Verma model [13], [14], [15]. The Page and Modified Page models have been mainly used for agricultural products, and they are not always suitable for use with heterogeneous household waste[16], [17], [18].

Advances in artificial intelligence (AI) have accelerated the development of deep learning architectures, with Long Short-Term Memory (LSTM) networks demonstrating superior performance in modelling temporal and sequential data[19]. Unlike empirical models, LSTM networks can also learn complex non-linear relationships and temporal dependencies. Gray forecasting models provide an effective approach for predicting waste generation with limited data, supporting efficient waste management and resource planning[20]. However, the risk of overfitting with small datasets, large data needs, and restricted physical interpretability plagues pure LSTM techniques. This drawback raises the possibility that hybrid models, which combine the flexibility of machine learning with the physical interpretation of empirical equations, may offer superior performance for drying kinetics modelling. Despite extensive research on drying kinetics, several gaps exist for household organic waste in developing economies:(1) Most studies focus on agricultural products or sewage sludge rather than household waste;(2) Limited application of advanced machine learning methods;(3) Absence of comprehensive model comparison using information criteria;(4) Lack of integrated energy-economic-environmental analysis.

2. EXPERIMENTAL METHODOLOGY

2.1 Collection and Characterization of Household Organic Waste

Household organic wet waste (HOWW) was sampled from an urban residential area in Maharashtra, India, during Jan-Feb 2025, following the sampling protocol of [11]. Manual sorting of 10 representative samples indicated that the waste consisted mostly of vegetable peels (45 ± 3%), cooked food leftovers (35 ± 2%), and fruit residues (20 ± 2%). To ensure particle- size uniformity, the waste was homogenized in the laboratory by a Philips HR7627/00 (700 W) blender for 2 minutes and stored in 2-l airtight containers at 4°C until use (max. 24 hours) to prevent any aggregation of the particles, loss of moisture, and microbial degradation. Figure 1 shows the waste preparation workflow.

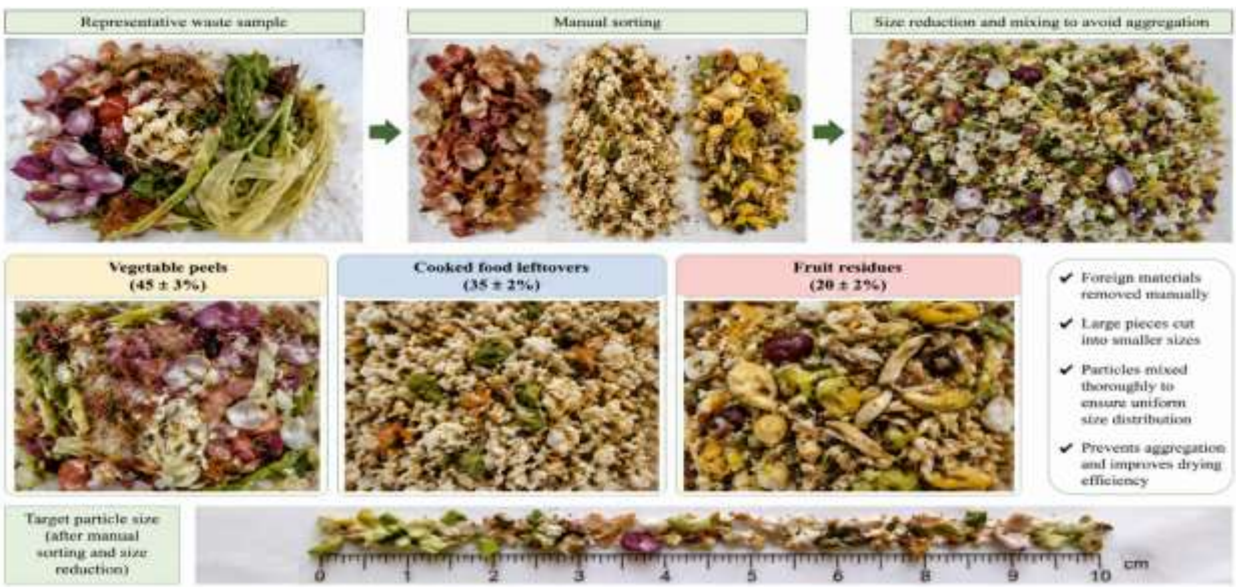

Figure 1. Manual Sorting and Particle Size Uniformity of Household Organic Waste

The organic waste samples were analysed in triplicate using the standard analytical procedures [21], and the results are referred to as "proximate analysis". The initial moisture content ranged from 68–75% (wet basis) and was determined using a Mettler

Toledo HR83 digital moisture analyzer at 105°C until equilibrium mass was reached (nearly 6 h). Total solids content ranged from 25 to 32%, and the volatile solids content accounted for 88 ± 2% of the dry matter. The pH of the homogenized waste was measured using a Hanna HI 2210 digital pH meter and was found to be 5.8 ± 0.3. The bulk density was determined using a graduated-cylinder method and was found to be 485 ± 15 kg m^{-3}.To ensure consistency among the experimental runs, the homogenized household organic wet waste was thoroughly mixed before each experiment, and representative portions were withdrawn for drying tests. The sample composition was maintained as closely as possible to the measured average composition of vegetable peels, cooked food residues, and fruit residues. The prepared samples were used within 24 h of collection and storage to minimize changes in moisture content and biological degradation. All physicochemical measurements were performed in triplicate, and the reported values represent the measured range or mean value with the corresponding variation.

2.2 Experimental Methodology

A completely randomized experimental design was adopted to evaluate the effect of drying temperature on the drying behavior of household organic wet waste. Three independent variables were studied: Drying temperature (70, 90, 100, 120, and 140°C), Air velocity (0.5, 1.0, and 1.5 m s^{-1}), and Sample thickness (5, 10, and 15 mm). The base experimental condition used for the systematic comparison of drying models was fixed at an air velocity of 1.0 m s^{-1} and a sample thickness of 10 mm. Additional experiments varied one parameter at a time while holding the other two at the base condition. The temperature range (70-140°C) was selected to cover both energy-efficient low-temperature drying and rapid high-temperature drying, and to permit reliable Arrhenius analysis.

The transitional drying temperature of 100 °C was selected because several studies on organic waste drying have reported it as an effective operating point [22], [23]. The study was conducted in triplicate (n = 3), yielding a total of 81runs: 45 at the base condition (5 temperatures × 3 replicates × 3 sampling times) and 36 additional runs (3 velocities × 3 thicknesses × 3 replicates) for parameter-variation studies. Sampling-time variation was achieved by adjusting the time resolution based on the drying stage. For the model-comparison experiments, the drying air temperature was maintained at the prescribed set point throughout each run, while the air velocity and sample thickness were maintained at 1.0 m s^{-1} and 10 mm, respectively. Approximately 100 ± 0.1 g of homogenized waste was uniformly distributed over the tray to obtain a relatively uniform drying layer. The drying experiments were continued until the sample mass approached a constant value. The measured mass loss at successive time intervals was used to calculate the moisture content and moisture ratio for model fitting. All experiments were conducted under the same loading and measurement procedure to ensure comparability among the drying temperatures.

2.3 Drying Equipment and Procedure.

All drying evaluations were performed using the developed drying system as a convective hot-air oven (Bio-Technics India, Model BT-29; Figure 2). The system was equipped with: A digital PID temperature controller (range 40-200°C, accuracy of ±1°C); Airflow was controlled between 0.3 and 3.0 m s^{-1}, with an accuracy of ±0.05 m s^{-1}, and the samples were put on a 20 × 20 cm stainless-steel mesh tray. Before each run, the empty tray was heated at the preset drying temperature for 30 min to establish thermal equilibrium (tare weight). A homogenized sample of approximately 100 ± 0.1 g was evenly spread on the drying tray to achieve the desired layer thickness. The sample was placed in the hot air oven, and mass was recorded on a Sartorius BSA2202S digital balance (accuracy ±0.01 g) at the following intervals: Mass measurements were taken at 5 min intervals for the first 60 min, every 10 min from 60 to 120 min, and every 30 min thereafter until the sample reached a constant mass. Sample surface temperature was monitored using a Fluke 62 MAX+ infrared thermometer, and air velocity at the sample position was verified using a Testo 425 hot-wire anemometer to confirm stable operating conditions. Before introducing the sample, the drying chamber was allowed to reach thermal equilibrium at the selected temperature. The initial sample mass was recorded immediately before the start of drying and subsequent mass measurements were performed without changing the sample loading arrangement. The drying air velocity was verified at the sample location before and during the experiments. This procedure was followed for all temperature conditions to minimize variations arising from equipment warm-up, sample loading, and airflow conditions.

Figure 2. Laboratory conventional hot-air drying setup used for drying experiments

2.4 Moisture Content Measurement and Moisture Ratio Computation

The moisture content (M) of household organic waste (HOWW) at any drying time t was determined as[24]:

$$M_t = \frac{m_t - m_{dry}}{m_{dry}} \text{(kg water / kg dry matter)} \quad (1)$$

where m_t is the sample mass at drying time t and $m_{dry}$is the oven-dry mass of the sample.

The moisture ratio (MR) was defined as[25]:

$$MR = \frac{M_t - M_e}{M_0 - M_e} \quad (2)$$

where M_e is the equilibrium moisture content. Because the initial moisture content of HOWW (68–75% w.b.) was much greater than M_e(< 2% d.b. for the studied conditions), the term $M_e$was considered negligible, and the simplified form was used [25]:

$$MR = \frac{M_t}{M_0} \quad (3)$$

Where, (M_t)represents the moisture content at drying time (t), $(M_0)$is the initial moisture content, and$(M_e)$is the equilibrium moisture content. The moisture content was expressed on a dry basis for calculation of the moisture ratio. The general expression for moisture ratio is $(MR = (M_t - M_e)/(M_0 - M_e))$. Since the equilibrium moisture content under the experimental drying conditions was less than 2% (dry basis) and was substantially smaller than the initial moisture content, $(M_e)$was considered negligible. Therefore, the simplified expression $(MR = M_t/M_0)$ was used for subsequent thin-layer model fitting. The same definition was applied consistently to all drying temperatures.

The drying rate (DR) was calculated using a discrete time-difference formulation:

$$DR = \frac{M_t - M_{t+\Delta t}}{\Delta t} \text{ (kg moisture kg}^{-1} \text{ dry solids min}^{-1}\text{)} \quad (4)$$

where $M_t$and $M_{t+\Delta t}$are the moisture contents at consecutive observation times t and $t + \Delta t$.

2.5 Model Fitting Statistical Analysis

Eight semi-empirical thin-layer drying models were fitted to the moisture ratio data using nonlinear least-squares regression implemented in MATLAB R2024a with the Levenberg–Marquardt algorithm, as implemented in the lsqcurvefit function. The objective function minimized the sum of squared residuals (SSR):

$$SSR = \sum_{i=1}^{n} (y_i - \bar{y}\text{i})^2 \quad (5)$$

Physically meaningful parameter bounds were imposed to prevent non-physical estimates: $0.0001 \leq k \leq 0.1 min^{-1}, 0.8 \leq n \leq 2.0, and 0.8 \leq a \leq 1.2.$Initial parameter values were obtained from linearized forms of the models, and convergence was assumed when relative changes in SSR between iterations fell below 10^{-8}.

The eight evaluated models are listed in Table 1, with all equations verified against canonical references [26], [27].

Table 1. This study assessed semi-empirical thin-layer drying models.

No.	Model Name	Model Equation	Parameters
1	Newton (Lewis)	$MR = exp(-kt)$	k
2	Henderson-Pabis	$MR = a.exp(-k.t)$	a, k
3	Page	$MR = exp(-kt^n)$	k, n
4	Logarithmic	$MR = exp(-(k\ t)n)$	a, k, c
5	Midilli-Kucuk	$MR = exp(-(k\ t)n)$	a, k, n, b
6	Verma	$MR = a\ exp(-kt) + (1 - a)\ exp(-gt)\ t$	a, k, g
7	Wang-Singh	$MR = 1 + at + bt^2$	a, b
8	Two-Terms	$MR = a.exp(-(k\ t)n)$	a, b, k_1, k_2

The model parameters are defined as follows: MR is the dimensionless moisture ratio; k, k_1, and $k_2$are drying rate constants with units of reciprocal time (s^{-1} or $\min^{-1}$); $a$and $b$are dimensionless scaling coefficients; and $n$is a dimensionless empirical exponent. The selected time unit should remain consistent throughout the analysis, particularly when reporting the drying constants and calculating the effective moisture diffusivity. The performance of each model was assessed using five statistical criteria:

$$R^2 = \frac{\sum_{i=1}^{n} (y_i - \hat{y_i})^2}{\sum_{i=1}^{n} (y_i - \bar{y}\text{i})^2} \quad (6)$$

$$RSME = \left[\frac{1}{N} \sum_{i=1}^{N} (y_i - \bar{y}\text{i})^2\right]^{\frac{1}{2}} \quad (7)$$

$$X^2 = \sum_{i=1}^{n} \frac{(y_i - \bar{y}\text{i})^2}{\bar{y}\text{i}} \quad (8)$$

$$AIC = N \ln\left(\frac{SSR}{N}\right) + 2_p \quad (9)$$

$$BIC = N \ln\left(\frac{SSR}{N}\right) + p \ln(N) \quad (10)$$

In these equations, Ndenotes the number of experimental annotations, while p represents the number of fitted model parameters. The terms $MR_{\text{exp}}$and MR_{pred} correspond to the experimental and model-predicted moisture ratios, respectively. Model comparison was performed using a combination of goodness of fit and information-theoretic criteria. Specifically, R^2, RMSE, χ^2, AIC, and BIC were computed for each model; preference was given to the model exhibiting the strongest agreement with the experimental data, characterized by the largest $R^2$and the smallest values of the remaining statistical indices.

2.6 Determination of Effective Moisture Diffusivity

The effective moisture diffusion coefficient was calculated using Fick's second law of diffusion. For thin-layer drying, the analytical solution proposed by Crank was employed to describe moisture movement within the materials[28]:

$$\left[MR = \frac{8}{\pi^2}\sum_{n=0}^{\infty}\frac{1}{(2n+1)^2}\exp\left[-\frac{(2n+1)^2\pi^2 D_{eff}t}{4L^2}\right]\right] \tag{11}$$

In this equation, MRdenotes the moisture ratio, $D_{\text{eff}}(\text{m}^2\ \text{s}^{-1})$represents the effective moisture diffusivity, t(s) is the drying time, and L(m) corresponds to the half-thickness of the drying sample.

For an extended drying period $(MR < 0.6)$,the higher-order terms of the analytical series become negligible. Consequently, only the first term of the series was retained, leading to the following simplified expression:

$$\left[\ln(MR) = \ln\left(\frac{8}{\pi^2}\right) - \frac{\pi^2 D_{eff}}{4L^2}t\right] \tag{12}$$

The value of $(D_{eff})$is obtained from the slope of the linear connection between $\ln(MR)$ and drying time using data from the falling-rate drying period $(MR < 0.6)$.

$$Slope = \frac{\pi^2 \times D_{eff}}{4L^2} \tag{13}$$

An Arrhenius-type equation may be used to illustrate the relationship between the drying state and the computed effective diffusivity values:

$$D_{eff} = D_0 \times exp\frac{-E_a}{RT} \tag{14}$$

In these models, D_0 denote the pre-exponential factor $\left(\frac{\text{m2}}{\text{s}}\right)$,Ea represent the activation energy $\left(\frac{\text{kJ}}{\text{mol}}\right)$, R represent the Universal gas constant $\left(\frac{\text{kJ}}{\text{mol}}\text{K}\right)$, and T is the absolute temperature (K)

Altering the latter expression to a logarithmic form and drawing a figure of ln $Deff$ against $\frac{1}{T}$, The y-axis intercept and the line's slope can be used to compute $D_0$and E_a, respectively. In the case of $1/T$, the measurable factor D_0 and $E_a$can be found by intersecting the y-axis and the line's slope. The effective moisture diffusivity (D_{eff}) was estimated separately for each drying temperature using the experimental moisture-ratio data from the falling-rate drying period. The waste layer was treated as a plane slab with negligible moisture transfer resistance at the exposed surface and approximately uniform initial moisture distribution. For sufficiently long drying times, the first term of the analytical series solution was retained. Taking the natural logarithm of the resulting expression gives a linear relationship between $\ln(MR)$and drying time. The slope of this linear regression was used to calculate D_{eff}according to Eq. (13), with the characteristic diffusion length taken as the half-thickness of the sample layer. The same procedure was applied to the experimental data obtained at each drying temperature.

2.7 Activation Energy (Arrhenius Analysis)

The Arrhenius equation was used to model how drying temperature affected D_{eff}:

$$\left[D_{eff} = D_0\, exp\left(-\frac{E_a}{RT}\right)\right] \tag{15}$$

D_0 is the pre-exponential factor, $E_a$is activation energy,$R = 8.314J/(mol \cdot K)$,and $T$is absolute temperature. Linearized form[29]:

$$ln(D_{eff}) = ln(D_0) - \frac{E_a}{R}\cdot\frac{1}{T} \tag{16}$$

Where the activation energy $(E_a)$and the pre-exponential factor (D_0) were estimated from the linear Arrhenius relationship, where the slope and intercept of the plot of $ln(Deff)$versus $1/T$ correspond to $E_a$and D_0 respectively. The activation energy was determined from the temperature dependence of the effective moisture diffusivity. The calculated D_{eff}values at the five drying temperatures were related to the absolute temperature using the Arrhenius equation. A plot of $\ln(D_{\text{eff}})$against $1/T$was fitted using linear regression. From the linearized Arrhenius equation, the slope was used to determine the activation energy (E_a), while the intercept was used to estimate the pre-exponential factor (D_0). Temperature was expressed in Kelvin for the Arrhenius analysis. The coefficient of determination of the linear fit was used to assess the adequacy of the Arrhenius relationship.

2.8 Energy Analysis

The specific energy consumption (SEC) was assessed as:

$$SEC = \frac{Q_{total}}{m_{water\ evaporated}}\ (MJ\ kg^{-1}\ water) \tag{17}$$

where Q_{total} denotes the cumulative thermal energy delivered to the drying chamber during the experiment, while m_{water}(kg) represents the amount of moisture removed from the materials. The value of Q_{total} was determined by integrating the oven power consumption over the entire drying period. The energy efficiency $(\eta)$was determined as the ratio of the theoretical latent heat required for water evaporation (2.26 MJ kg^{-1}) to the measured specific energy consumption (SEC).

3. RESULT AND DISCUSSION

3.1 Waste Characterization

The proximate analysis of HOWW (Table 2) confirms that the waste is a high-moisture, biodegradable substrate with high volatile-solids content, making it suitable for biological and thermochemical valorization after drying. The pH (5.8 ± 0.3) is within the optimal range for anaerobic digestion and composting. The bulk density (485 ± 15 kg m^{-3}) is consistent with values reported for mixed food waste [7], [8].

Table 2. Proximate characterization of household organic wet waste (HOWW).

Parameter	Value	Method
Moisture content (w.b.)	68–75%	Gravimetric, 105 °C, 6 h
Total solids (w.b.)	25–32%	Calculated
Volatile solids (% of dry matter)	88 ± 2%	550 °C, 2 h
pH	5.8 ± 0.3	Hanna HI 2210
Bulk density	485 ± 15 kg m^{-3}	Graduated cylinder

3.2 Analysis of Drying Kinetics and Curves

The moisture-ratio curves at the five drying temperatures are displayed in Figure 3. As expected, MR decreased continuously with time, and the rate of decrease became more pronounced at higher temperatures. At 70 °C, drying to MR = 0.05 required approximately 480 min, whereas at 140 °C the same endpoint was reached in approximately 95 min, a 5-fold reduction in drying time.

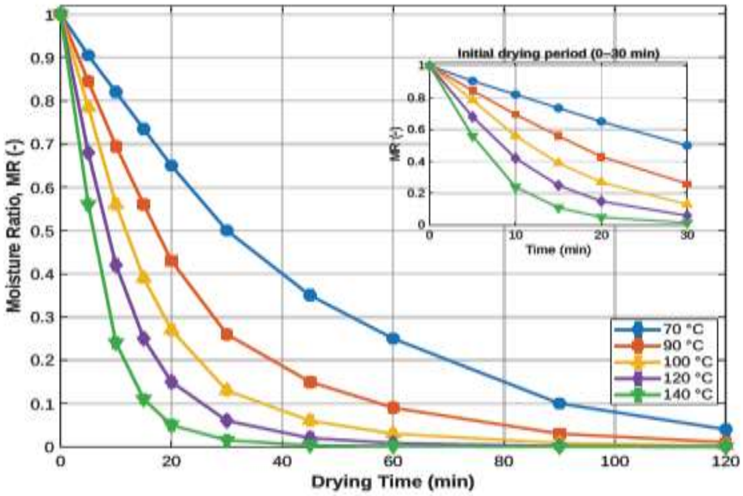

Figure 3. Experimental moisture ratio (MR) curves of household organic wet waste dried at 70, 90, 100, 120, and 140 °C. The inset shows the initial drying period (0–30 min).

3.3 Semi-Empirical Model Fittings

Experimental MR data for the five temperatures were fit to the eight models. The fit results of the 70 °C are given in detail in Table 3, and the fit results of the best-performing model (Midilli–Kucuk) at all five temperatures are summarized in Table 4. All the parameter sets and fit statistics for all eight models and all temperatures are provided in Supplementary Material (Tables S1–S5).

Table 3. Statistical performance of the eight thin-layer drying models for HOWW at 70 °C.

Rank	Drying Model	R^2	RMSE	χ^2 ($\times10^{-5}$)	AIC	BIC
1	Midilli–Kucuk	0.9996	0.0071	7.21	-120.77	-118.51
2	Page	0.9995	0.0077	7.03	-122.49	-121.36
3	Verma	0.9982	0.0154	30.98	-102.45	-100.75
4	Two-Term	0.9982	0.0154	31.02	-102.43	-100.74
5	Logarithmic	0.9977	0.0174	39.53	-99.28	-97.58
6	Henderson–Pabis	0.9967	0.0209	51.43	-96.62	-95.49
7	Newton (Lewis)	0.9954	0.0247	66.01	-94.24	-93.68
8	Wang–Singh	0.9398	0.0895	946.87	-58.75	-57.62

Each exponential type model produced $R^2 > 0.995$, which proved that each of these models was effectively used to define the drying method. Based on the combined statistical evaluation, the Midilli–Kucuk model provided the most reliable representation of the experimental drying behaviour, exhibiting the highest coefficient of determination R^2 together with the lowest RMSE and χ^2 values. The Page model was the most parsimonious (lowest AIC and BIC) because it uses only two parameters. Further models such ```as Verma, Two-Term, and Logarithmic models also showed good R^2 values ($R^2 > 0.997$). As for the Wang–Singh polynomial model, the results indicated that the best match was achieved ($R^2 = 0.9398$), which was a confirmation that the polynomial form is not suitable for describing the decrease of moisture content in convective drying.

Table 4. Midilli–Kucuk model parameters and fit statistics for HOWW at five drying temperatures (n = 3, base condition: 1.0 m s⁻¹, 10 mm).

T (°C)	a (×10⁻³ std. err.)	k (×10⁻³ std. err., min⁻¹)	n (×10⁻³ std. err.)	b (×10⁻⁴ std. err., min⁻¹)	n (×10⁻³ std. err.)	R^2	RMSE	χ^2 (×10⁻⁴)
70	0.9998 (3.2)	0.1021 (2.1)	1.052 (4.5)	0.100 (0.8)	1.052 (4.5)	0.9996	0.0071	0.72
90	0.9997 (2.9)	0.1582 (1.8)	1.081 (3.8)	0.118 (0.7)	1.081 (3.8)	0.9994	0.0078	0.87
100	0.9995 (2.6)	0.2151 (1.6)	1.103 (3.4)	0.142 (0.7)	1.103 (3.4)	0.9992	0.0083	0.95
120	0.9993 (2.3)	0.3276 (1.4)	1.128 (3.0)	0.171 (0.6)	1.128 (3.0)	0.9989	0.0089	1.04
140	0.9990 (2.0)	0.5669 (1.2)	1.152 (2.6)	0.205 (0.5)	1.152 (2.6)	0.9987	0.0094	1.12

The moisture transport was found to be strongly dependent on temperature, as the drying constant k of the Midilli–Kucuk model increased from 0.1021 to 0.5669 min-1 with increasing temperature from 70 to 140 °C. With an increase in temperature, the exponent n rose slightly from 1.05 to 1.15, thus showing a small deviation from the first-order reaction. The parameter b, representing the linear-time term that captures the asymptotic approach to equilibrium, increased from 0.0001 to 0.0002 min⁻¹, consistent with more rapid equilibration at higher temperatures.

3.4 Effective Moisture Diffusivity

The $D_eff$values (Table 5) increased from 4.70×10^{-9} to $2.60 \times 10^{-8} m^2 s^{-1}$as temperature increased from 70 to 140 °C-a 5.5-fold increase. The study stated ranges in the literature for food and organic waste drying $(10^{-9} to 10^{-7} m^2 s^{-1}) (Beigi\ et\ al., 2020;\ Wang\ et\ al., 2014)$.Arrhenius equation$(R^2 = 0.997)$ provides a good description of the temperature dependency, confirming that moisture diffusion in HOWW is a thermally activated process.

Table 5. Effective moisture diffusivity and Arrhenius parameters for HOWW at 1.0 m s⁻¹ and 10 mm sample thickness.

Drying Temperature (°C)	Temperature (K)	Effective Moisture Diffusivity, D_{eff}(×10⁻⁹ m²/s)	$\ln(D_{eff})$	$1/T$(×10⁻³ K⁻¹)
70	343.15	4.70	-19.176	2.914
90	363.15	7.20	-18.749	2.754
100	373.15	9.80	-18.441	2.680
120	393.15	15.00	-18.015	2.544
140	413.15	26.00	-17.465	2.420

3.5 Activation Energy

The Arrhenius analysis (Figure 4) produced a pre-exponential factor and activation energy of $E_a = 27.22 kJmol^{-1}$ and $D_0 = 6.28 \times 10^{-5} m^2 s^{-1}$($R^2$ = 0.997). This $E_a$is within the range reported for similar organic substrates: 18.0–32.5 kJ mol⁻¹ for food waste, $22.7 - 29.1 kJmol^{-1}$for sewage sludge [30], and $24.4 - 33.6 kJmol^{-1}$for fruit peels [32]. The value indicates that moisture removal in HOWW is a moderately energy-intensive diffusion-controlled process, with energy barriers consistent with the breaking of capillary and hydrogen bonds in the heterogeneous waste matrix.

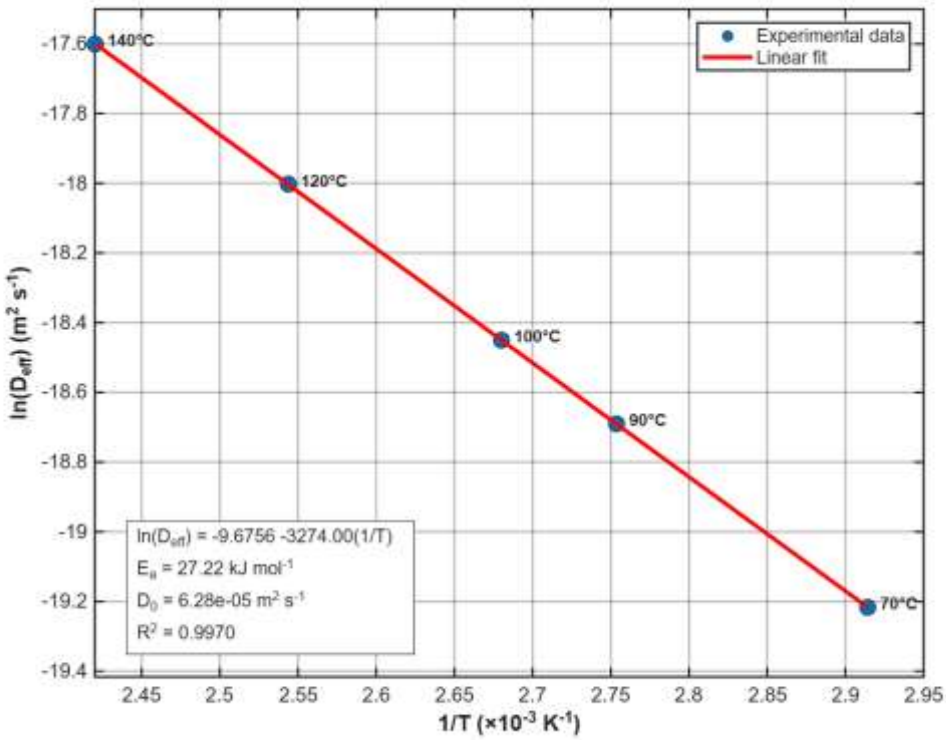

Figure 4. Arrhenius plot of effective moisture diffusivity (D_{eff}) for household organic wet waste during convective hot-air drying, showing the linear fit with $E_a = 27.22$kJ mol-1, $D_0 = 6.28 \times 10^{-5}$m2 s-1, and $R^2 = 0.997$.

3.6 Energy Analysis

Table 6 summarizes the total drying time, total energy used, and specific energy consumption(SEC) for each temperature.

Table 6. Energy analysis for drying of waste at 1.0 m s^{-1} and 10 mm thickness.

T (°C)	Drying time (min)	Energy consumed (MJ)	Water evaporated (kg)	SEC (MJ kg^{-1} water)	Energy consumed (MJ)	Water evaporated (kg)
70	480	5.89	0.71	8.30	5.89	0.71
90	285	4.16	0.72	5.78	4.16	0.72
100	220	3.50	0.72	4.86	3.50	0.72
120	145	3.10	0.72	4.31	3.10	0.72
140	95	2.89	0.71	4.07	2.89	0.71

SEC decreased monotonically with temperature from 8.30 MJ kg^{-1} (70 °C) to 4.07 MJ kg^{-1} (140 °C). However, drying at 140 °C caused visible browning and a reduction in volatile solids retention (83.1% vs. 86.4% at 100 °C), as well as increased odor generation. Drying at 100 °C offered the best overall balance among drying time (220 min), SEC (4.86 MJ kg^{-1}), and product quality (volatile solids retention of 86.4% and no visible discoloration). The non-linear relationship between SEC and temperature is consistent with the findings of similar organic substrates[33].

3.7 Comparison with Literature

A comparison of D_eff and E_a values with literature data for similar organic materials is presented in Table 7. While E_a is consistent with values reported for sewage sludge and food waste, the D_eff values obtained in this investigation fall within the range reported for mixed food waste and fruit residues. This consistency supports the validity of the experimental and analytical procedures used.

Table 7. Comparison of D_eff and E_a values with literature data for similar organic materials.

Material	$Trange(°C)$	D_eff (m² s⁻¹)	$E_a(kJmol^{-1})$	Source
Mixed food waste	50–80	1.0×10^{-9} to 5.0×10^{-9}	22.5	[31]
Sewage sludge	80–140	5.2×10^{-10} to 2.8×10^{-8}	25.1	[30]
Fruit peels (apple)	50–90	2.4×10^{-9} to 1.1×10^{-8}	28.9	[32]
Vegetable waste	60–100	3.1×10^{-9} to 1.2×10^{-8}	26.4	[34]
HOWW (this study)	70–140	4.7×10^{-9} to 2.6×10^{-8}	27.2	—

3.8 Implications and Limitations

The high performance of the Midilli–Kucuc model indicates that the drying characteristics of the heterogeneous household wastes can be well simulated by using a relatively simple four-parameter equation, which is good and encouraging for scale-up and process design. The optimum temperature identified (100°C) will prove to be a practical operating value for decentralized drying systems in the context of Indian cities. There are a number of caveats that should be noted. The experiments were carried out at laboratory scale and with thin layers (≤15 mm), which may have different kinetics for thick-bed and/or rotary drying in industry. Second, there were some differences in waste composition across seasons (e.g., more fruit in summer, affecting generalizability). Third, the model parameters were optimized based on one batch of waste, and future work should verify the model with other batches of waste throughout seasons. Fourth, it was assumed that the oven would operate in a steady state during the energy analysis; this could result in an underestimate of SEC by 5-10%.

4. CONCLUSIONS

The convective hot-air drying process of HOWW was studied using 8 semi-empirical thin-layer drying models at 5 drying temperatures (70, 90,100,120, and 140 °C). The Midilli–Kucuk model showed the best predictive accuracy across all drying conditions, with coefficients of determination (R^2) values greater than 0.9987 and RMSE values less than or equal to 0.0094, and the Page model was simpler and more reliable. On the other hand, the Wang–Singh polynomial model was shown to be unsuitable to represent the drying behavior of HOWW. The effective moisture diffusivity (D_eff) increased from 4.70×10^{-9} to 2.60×10^{-8} m² s⁻¹ with the increase of drying temperature, showing good Arrhenius correlation ($R^2 = 0.997$) with the activation energy (E_a) of 27.22 $kJmol^{-1}$ and the pre-exponential factor (D_0) of $6.28 \times 10^{-5} m^2 s^{-1}$. Under the conditions studied, the optimum drying temperature was found to be 100 °C with a drying time of 220 min, volatile solids retention of 86.4%, and an energy consumption of 4.86 MJ kg-1 water removed. The study also revealed that the air velocity from 0.5 m s⁻¹ to 1.5 m s⁻¹ decreased the drying time. The drying times were almost doubled by increasing the sample thickness from 5 to 15 mm; however, due to higher moisture transfer resistance, there was only a marginal increase in drying time beyond 1.2 m s⁻¹. The results have shown that the Midilli–Kucuk model is a reliable model for the design, optimisation and control of decentralised organic waste drying systems from household waste to enable circular economy applications like composting, anaerobic digestion and bioenergy production. Future investigations should further confirm the proposed model by testing it in pilot-scale rotary and fluidized-bed dryers, incorporating renewable energy sources like solar and biomass to lower specific energy use, carrying out techno-economic and life cycle evaluation, and creating hybrid empirical machine learning models to further improve prediction accuracy and process optimization.

ACKNOWLEDGEMENTS

The authors declare that no funds, grants, or other support were received during the preparation of this manuscript.

AUTHOR CONTRIBUTIONS

Punam Bundele: Writing, Methodology, Laboratory Analysis, Formal Analysis, Conceptualization, Investigation

Marshiana D.: Formal Analysis, Supervision, Review & Editing.

Adeline Sneha J: Supervision

CONFLICT OF INTEREST

The authors declare that there is no conflict of interest.

ETHICS STATEMENT

Ethical approval was not required for this study.

DATA AVAILABILITY STATEMENT

Data supporting the findings of this study are available from the corresponding author upon reasonable request.

REFERENCES

[1] S. Kaza, L. C. Yao, P. Bhada-Tata, F. Van Woerden, and D. Levine, "What a Waste 2.0: A Global Snapshot of Solid Waste Management to 2050," *What a Waste 2.0: A Global Snapshot of Solid Waste Management to 2050*, Sep. 2018, doi: 10.1596/978-1-4648-1329-0.

[2] P. Shukla, P. K. Sharma, S. Pandey, and V. Chintala, "Unsegregated Municipal Solid Waste in India-Current Scenario, Challenges and Way Forward", doi: 10.46488/NEPT.2021.v20i02.048.

[3] M. Madhavaraj and K. Karthikeyan, "A review of municipal solid waste management and landfills in India: environmental impacts, sustainable strategies and policy insights," *J. Mater. Cycles Waste Manag.*, pp. 1–24, Jun. 2025, doi: 10.1007/S10163-025-02287-4/METRICS.

[4] P. Bundele and M. Devaerakkam, "A Comprehensive Assessment to Harness Artificial Intelligence Technology in the Organic Waste Management of Urban India," *Challenges in Sustainability*, vol. 13, no. 3, pp. 459–476, Sep. 2025, doi: 10.56578/CIS130310.

[5] E. E. Manea, C. Bumbac, L. R. Dinu, M. Bumbac, and C. M. Nicolescu, "Composting as a Sustainable Solution for Organic Solid Waste Management: Current Practices and Potential Improvements," Aug. 01, 2024, *Multidisciplinary Digital Publishing Institute (MDPI)*. doi: 10.3390/su16156329.

[6] I. E. Karadirek, O. Erkaya, and A. S. Ciggin, "Comparative life cycle assessment of sewage sludge drying by solar and thermal drying technologies," *Waste Management*, vol. 201, p. 114826, Jun. 2025, doi: 10.1016/J.WASMAN.2025.114826.

[7] W. Senadeera, B. R. Bhandari, G. Young, and B. Wijesinghe, "Influence of shapes of selected vegetable materials on drying kinetics during fluidized bed drying," *J. Food Eng.*, vol. 58, no. 3, pp. 277–283, Jul. 2003, doi: 10.1016/S0260-8774(02)00386-2.

[8] R. Mieldažys, E. Jotautienė, A. Pocius, and A. Jasinskas, "Analysis of organic agricultural waste usage for fertilizer production," *Agronomy Research*, vol. 14, no. 1, pp. 143–149, 2016.

[9] S. M. Kang *et al.*, "Effects of Organic Fertilizer Mixed with Food Waste Dry Powder on the Growth of Chinese Cabbage Seedlings," *Environments 2021, Vol. 8, Page 86*, vol. 8, no. 8, p. 86, Aug. 2021, doi: 10.3390/ENVIRONMENTS8080086.

[10] S. V Gokhale and S. S. Lele, "Dehydration of Red Beet Root (Beta vulgaris) by Hot Air Drying: Process Optimization and Mathematical Modeling," *Food Sci. Biotechnol*, vol. 20, no. 4, pp. 955–964, 2011, doi: 10.1007/s10068-011-0132-4.

[11] I. Tryhuba *et al.*, "An Approach to Assessing the State of Organic Waste Generation in Community Households Based on Associative Learning," *Sustainability 2023, Vol. 15, Page 15922*, vol. 15, no. 22, p. 15922, Nov. 2023, doi: 10.3390/SU152215922.

[12] L. M. Bal, S. Satya, and S. N. Naik, "Solar dryer with thermal energy storage systems for drying agricultural food products: A review," *Renewable and Sustainable Energy Reviews*, vol. 14, no. 8, pp. 2298–2314, Oct. 2010, doi: 10.1016/J.RSER.2010.04.014.
[13] R. B. Keey, T. A. G. Langrish, and J. C. F. Walker, "Moisture Diffusion," pp. 85–115, 2000, doi: 10.1007/978-3-642-59653-7_5.
[14] J. S. Mahesh, B. Rengaraju, and S. Selvakumarasamy, "Effect of ANN and semi-empirical models on dried Annona muricata leaves," *Biomass Conversion and Biorefinery 2024 15:4*, vol. 15, no. 4, pp. 6223–6235, Apr. 2024, doi: 10.1007/S13399-024-05546-W.
[15] W. P. da Silva, C. M. D. P. S. e Silva, F. J. A. Gama, and J. P. Gomes, "Mathematical models to describe thin-layer drying and to determine drying rate of whole bananas," *Journal of the Saudi Society of Agricultural Sciences*, vol. 13, no. 1, pp. 67–74, Jan. 2014, doi: 10.1016/J.JSSAS.2013.01.003.
[16] E. K. Akpinar, "Determination of suitable thin layer drying curve model for some vegetables and fruits," *J. Food Eng.*, vol. 73, no. 1, pp. 75–84, Mar. 2006, doi: 10.1016/J.JFOODENG.2005.01.007.
[17] A. Vega-GÁlvez, M. Miranda, C. Bilbao-SÁinz, E. Uribe, and R. Lemus-Mondaca, "EMPIRICAL MODELING OF DRYING PROCESS FOR APPLE (CV. GRANNY SMITH) SLICES AT DIFFERENT AIR TEMPERATURES," *J. Food Process. Preserv.*, vol. 32, no. 6, pp. 972–986, Dec. 2008, doi: 10.1111/J.1745-4549.2008.00227.X.
[18] R. Kumar, P. Kumar, N. K. Hota, and O. P. Pandey, "Semi-empirical thin-layer drying model for the agricultural products," *Chem. Eng. Commun.*, vol. 212, no. 5, pp. 728–738, 2025, doi: 10.1080/00986445.2024.2432672.
[19] II. Pyrka, N. N.- Foods, and undefined 2025, "Thin-Layer, Intermittent, Near-Infrared Drying of Two-Phase Olive Pomace: Mathematical Modeling and Effect on Recovery of Bioactive Compounds and," *mdpi.comI Pyrka, N NenadisFoods, 2025•mdpi.com*, Accessed: Dec. 08, 2025. [Online]. Available: https://www.mdpi.com/2304-8158/14/12/2042
[20] M. Anjum, S. Shahab, and M. S. Umar, "Application of Modified Grey Forecasting Model to Predict the Municipal Solid Waste Generation using MLP and MLE," *Application of Modified Grey Forecasting Model to Predict the Municipal Solid Waste Generation using MLP and MLE*, vol. 6, no. 5, pp. 1276–1296, Aug. 2021, doi: 10.33889/IJMEMS.2021.6.5.077.
[21] C. Ertekin and M. Z. Firat, "A comprehensive review of thin-layer drying models used in agricultural products," *Crit. Rev. Food Sci. Nutr.*, vol. 57, no. 4, pp. 701–717, Mar. 2017, doi: 10.1080/10408398.2014.910493;REQUESTEDJOURNAL:JOURNAL:BFSN20.
[22] C. L. Hii, C. L. Law, and M. Cloke, "Modeling using a new thin layer drying model and product quality of cocoa," *J. Food Eng.*, vol. 90, no. 2, pp. 191–198, Jan. 2009, doi: 10.1016/J.JFOODENG.2008.06.022.
[23] D. I. Onwude, N. Hashim, R. B. Janius, N. M. Nawi, and K. Abdan, "Modeling the Thin-Layer Drying of Fruits and Vegetables: A Review," *Compr. Rev. Food Sci. Food Saf.*, vol. 15, no. 3, pp. 599–618, May 2016, doi: 10.1111/1541-4337.12196; PAGEGROUP:STRING:PUBLICATION.
[24] R. Kumar, O. P. Pandey, S. K. Dhiman, and P. Kumar, "Influence of Blanching and Drying Air Temperature on Drying Kinetics of Banana Slices," *Journal of Biosystems Engineering 2021 46:4*, vol. 46, no. 4, pp. 375–385, Nov. 2021, doi: 10.1007/S42853-021-00114-W.
[25] M. Beigi, "Thin layer drying of wormwood (Artemisia absinthium L.) leaves: dehydration characteristics, rehydration capacity and energy consumption," *Heat and Mass Transfer 2017 53:8*, vol. 53, no. 8, pp. 2711–2718, Mar. 2017, doi: 10.1007/S00231-017-2018-3.
[26] I. Alibas and A. Yilmaz, "Microwave and convective drying kinetics and thermal properties of orange slices and effect of drying on some phytochemical parameters," *Journal of Thermal Analysis and Calorimetry 2021 147:15*, vol. 147, no. 15, pp. 8301–8321, Nov. 2021, doi: 10.1007/S10973-021-11108-3.
[27] J. Crank, "THE MATHEMATICS OF DIFFUSION CLARENDON PRESS OXFORD 1975".
[28] I. Pyrka, N. N.- Foods, and undefined 2025, "Thin-Layer, Intermittent, Near-Infrared Drying of Two-Phase Olive Pomace: Mathematical Modeling and Effect on Recovery of Bioactive Compounds and," *mdpi.comI Pyrka, N NenadisFoods, 2025•mdpi.com*, Accessed: Aug. 01, 2026. [Online]. Available: https://www.mdpi.com/2304-8158/14/12/2042
[29] B. Budianto, "Thermal sensitivity of moisture diffusion and lipid oxidation during drying of Citrus maxima seeds," *Heat and Mass Transfer 2026 62:6*, vol. 62, no. 6, pp. 74-, May 2026, doi: 10.1007/S00231-026-03700-W.
[30] H. L. Wang *et al.*, "The thin-layer drying characteristics of sewage sludge by the appropriate foaming pretreatment.," *Water Science and Technology*, vol. 69, no. 9, pp. 1859–1866, 2014, doi: 10.2166/WST.2014.093.

[31] M. Beigi, M. Torki, F. Khoshnam, and M. Tohidi, "Thermodynamic and environmental analyses for paddy drying in a semi-industrial dryer," *Journal of Thermal Analysis and Calorimetry 2020 146:1*, vol. 146, no. 1, pp. 393–401, Jun. 2020, doi: 10.1007/S10973-020-09968-2.

[32] A. Kaya, O. Aydin, and C. Demirtaş, "Drying Kinetics of Red Delicious Apple," *Biosyst. Eng.*, vol. 96, no. 4, pp. 517–524, Apr. 2007, doi: 10.1016/J.BIOSYSTEMSENG.2006.12.009.

[33] M. Stramarkou, T. V. Missirli, K. Kyriakopoulou, S. Papadaki, A. Angelis-Dimakis, and M. Krokida, "The Recovery of Bioactive Compounds from Olive Pomace Using Green Extraction Processes," *Resources 2023, Vol. 12, Page 77*, vol. 12, no. 7, p. 77, Jun. 2023, doi: 10.3390/RESOURCES12070077.

[34] T. Tultabayeva *et al.*, "Comparative Evaluation of Drying Methods for Vegetable Waste Aimed at Producing Natural Functional Food Ingredients," *Molecules 2026, Vol. 31, Page 1190*, vol. 31, no. 7, p. 1190, Apr. 2026, doi: 10.3390/MOLECULES31071190